

Supporting information 1 of:

Study of the pH effects on water-oil-illite interfaces by molecular dynamics

Authors

Anderson Arboleda-Lamus^a, Leonardo Muñoz-Rugeles^a, Jorge M. del Campo^b, Nicolas Santos-Santos^c and Enrique Mejía-Ospino^a

Corresponding autor

Enrique Mejia-Ospino

E-mail: emejia@uis.edu.co

Parameter to different systems simulated.

Table S1. Lennard-Jones and partial charge parameters of the illita (CLAYFF).

Atom type	Description	$\epsilon \left(\frac{kJ}{mol * \text{\AA}^2} \right)$	$\sigma(\text{\AA})$	$q(e)$
Alo		1.3298e-06	4.2712	1.5750
Alt		1.8405e-06	3.3020	1.5750
H		0.0000e00	0.0000	0.4250
K		1.0000e-01	3.3340	1.0000
Mgo		9.0298e-07	5.2643	1.3600
Ob		1.5540e-01	3.1655	-1.0500
Obos		1.5540e-01	3.1655	-1.1808
Obts		1.5540e-01	3.1655	-1.1688
Oeao		1.5540e-01	3.1655	-1.1875
Oeat		1.5540e-01	3.1655	-1.0688
Oest		1.5540e-01	3.1655	-0.9500
Oh		1.5540e-01	3.1655	-0.9500
Ohs		1.5540e-01	3.1655	-1.0808
Sit		1.8405e-06	3.3020	2.1000

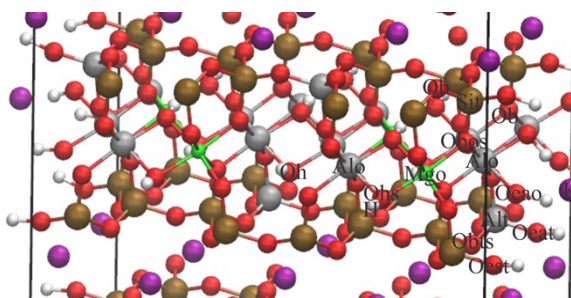


Table S2. Bond coefficients parameters of the illita (CLAYFF).

Bond type	$k_{r,ij} \left(\frac{kJ}{mol * \text{\AA}^2} \right)$	$r_{0,ij}(\text{\AA})$
H-Oeao	554.1350	1.0000
H-Oeat	554.1350	1.0000
H-Oest	554.1350	1.0000
H-Oh	554.1350	1.0000
H-Ohs	554.1350	1.0000

Table S3. Angle coefficients parameters of the illite (CLAYFF).

Angle type	$k_{\theta,ijk} \left(\frac{kJ}{mol * rad^2} \right)$	$\theta_{0,ijk}(deg)$
Alo-Oeao-H	30.0000	109.4700
Alo-Oh-H	30.0000	109.4700
Alo-Ohs-H	30.0000	109.4700
Alt-Oeat-H	30.0000	109.4700
H-Oest-Sit	30.0000	109.4700
H-O-Mgo	30.0000	109.4700

Table S4. Lennard-Jones and partial charge parameters of the water (CLAYFF).

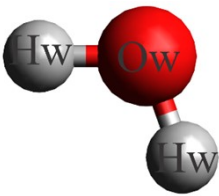
Atom type	Description	$\epsilon \left(\frac{kJ}{mol * \text{\AA}^2} \right)$	$\sigma(\text{\AA})$	$q(e)$
Hw		0.0000e-4	4.2712	1.5750
Ow		1.8405e-06	3.3020	1.5750

Table S5. Water's bond coefficients parameters (CLAYFF).

Bond type	$k_{r,ij} \left(\frac{kJ}{mol * \text{\AA}^2} \right)$	$r_{0,ij}(\text{\AA})$
Hw-Ow	554.1349	1.0000

Table S6. Water's angle coefficients parameters (CLAYFF).

Angle type	$k_{\theta,ijk} \left(\frac{kJ}{mol * rad^2} \right)$	$\theta_{0,ijk}(deg)$
Hw-O2-Hw	45.7695	109.4700

Table S7. Lennard-Jones and partial charge parameters of the toluene (CGENFF).

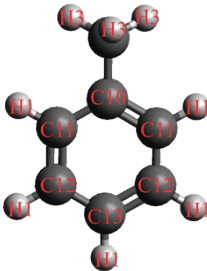
Atom type	Description	$\epsilon\left(\frac{kJ}{mol * \text{\AA}^2}\right)$	$\sigma(\text{\AA})$	$q(e)$
C10		7.0000e-02	3.5501	-0.0100
C11		7.0000e-02	3.5501	-0.1160
C12		7.0000e-02	3.5501	-0.1140
C13		7.0000e-02	3.5501	-0.1150
C3		7.8000e-02	3.6527	-0.2690
H1		3.0000e-02	2.4200	0.1150
H3		2.4000e-02	2.3876	0.0900

Table S8. Bond coefficients parameters of the toluene (CGENFF).

Bond type	$k_{r,ij}\left(\frac{kJ}{mol * \text{\AA}^2}\right)$	$r_{0,ij}(\text{\AA})$
C10-C11	305.0000	1.3750
C10-C3	230.0000	1.4900
C11-C12	305.0000	1.3750
C11-H1	340.0000	1.0800
C12-C13	305.0000	1.3750
C12-H1	340.0000	1.0800
C13-H1	340.0000	1.0800
C3-H3	322.0000	1.1110

Table S9. Angle coefficients parameters of the toluene (CGENFF).

Angle type	$k_{\theta,ijk}\left(\frac{kJ}{mol * rad^2}\right)$	$\theta_{0,ijk}(deg)$	$k_{UB,ik}\left(\frac{kJ}{mol * \text{\AA}^2}\right)$	$r_{0,ik}(\text{\AA})$
C10-C11-C12	40.0000	120.0000	35.0000	2.4162
C10-C11-H1	30.0000	120.0000	22.0000	2.1525
C10-C3-H3	49.3000	107.5000	0.0000	0.0000
C11-C10-C11	40.0000	120.0000	35.0000	2.4162
C11-C10-C3	45.8000	120.0000	0.0000	0.0000
C11-C12-C13	40.0000	120.0000	35.0000	2.4162
C11-C12-H1	30.0000	120.0000	22.0000	2.1525
C12-C11-H1	30.0000	120.0000	22.0000	2.1525
C12-C13-C12	40.0000	120.0000	35.0000	2.4162
C12-C13-H1	30.0000	120.0000	22.0000	2.1525
C13-C12-H1	30.0000	120.0000	22.0000	2.1525
H3-C3-H3	35.5000	108.4000	5.4000	1.8020

Table S10. Dihedral proper coefficients parameters of the toluene (CGENFF).

Dihedral proper type	$k_{\phi,ijkl} \left(\frac{kJ}{mol} \right)$	$n(adi.)$	$\delta_{0,ijkl}(deg)$	<i>Factorweight</i> (<i>adi.</i>)
C10-C11-C12-C13	3.1000	2.0000	180.0000	0.5000
C10-C11-C12-H1	4.2000	2.0000	180.0000	1.0000
C11-C10-C11-C12	3.1000	2.0000	180.0000	1.0000
C11-C10-C11-H1	4.2000	2.0000	180.0000	1.0000
C11-C10-C3-H3	0.0020	6.0000	0.0000	1.0000
C11-C12-C13-C12	3.1000	2.0000	180.0000	1.0000
C11-C12-C13-H1	4.2000	2.0000	180.0000	1.0000
C3-C10-C11-C12	3.1000	2.0000	180.0000	1.0000
C3-C10-C11-H1	2.4000	2.0000	180.0000	1.0000
H1-C11-C12-C13	4.2000	2.0000	180.0000	1.0000
H1-C11-C12-H1	2.4000	2.0000	180.0000	1.0000
H1-C12-C13-C12	4.2000	2.0000	180.0000	1.0000
H1-C12-C13-H1	2.4000	2.0000	180.0000	1.0000

Table S11. Lennard-Jones and partial charge parameters of the heptane (CGENFF).

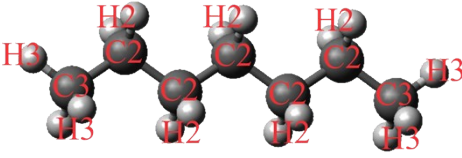
Atom type	Description	$\epsilon\left(\frac{kJ}{mol * \text{\AA}^2}\right)$	$\sigma(\text{\AA})$	$q(e)$
C2		5.6000e-02	3.5814	-0.1800
C3		7.8000e-02	3.6527	-0.2700
H2		3.5000e-02	2.3876	0.0900
H3		2.4000e-02	2.3876	0.0900

Table S12. Bond coefficients parameters of the heptane (CGENFF).

Bond type	$k_{r,ij}\left(\frac{kJ}{mol * \text{\AA}^2}\right)$	$r_{0,ij}(\text{\AA})$
C2-C2	222.5000	1.5300
C2-C3	222.5000	1.5280
C2-H2	309.0000	1.1110
C3-H3	322.0000	1.1110

Table S13. Angle coefficients parameters of the heptane (CGENFF).

Angle type	$k_{\theta,ijk}\left(\frac{kJ}{mol * rad^2}\right)$	$\theta_{0,ijk}(deg)$	$k_{UB,ik}\left(\frac{kJ}{mol * \text{\AA}^2}\right)$	$r_{0,ik}(\text{\AA})$
C2-C2-C2	58.3500	113.6000	11.1600	2.5610
C2-C2-C3	58.0000	115.0000	8.0000	2.5610
C2-C2-H2	26.5000	110.1000	22.5300	2.1790
C2-C3-H3	34.6000	110.1000	22.5300	2.1790
C3-C2-H2	34.6000	110.1000	22.5300	2.1790
H2-C2-H2	35.5000	109.0000	5.4000	1.8020
H3-C3-H3	35.5000	108.4000	5.4000	1.8020

Table S14. Dihedral proper coefficients parameters of the heptane (CGENFF).

Dihedral proper type	$k_{\varphi,ijkl}\left(\frac{kJ}{mol}\right)$	$n(adi.)$	$\delta_{0,ijkl}(deg)$	<i>Factorweight</i> (adi.)
C2-C2-C2-C2	0.1497	3.0000	180.0000	1.0000
C2-C2-C2-C3	0.0813	3.0000	180.0000	1.0000
C2-C2-C2-H2	0.1950	3.0000	0.0000	1.0000
C2-C2-C3-H3	0.1600	3.0000	0.0000	1.0000
C3-C2-C2-H2	0.1800	3.0000	0.0000	1.0000
H2-C2-C2-H2	0.2200	3.0000	0.0000	1.0000
H2-C2-C3-H3	0.1600	3.0000	0.0000	1.0000

Table S15. Lennard-Jones and partial charge parameters of the heptanoic acid (CGENFF).

Atom type	Description	$\epsilon \left(\frac{kJ}{mol * \text{\AA}^2} \right)$	$\sigma(\text{\AA})$	$q(e)$
C11		9.8000e-02	3.0291	0.8020
C21		5.6000e-02	3.5814	-0.1800
C22		5.6000e-02	3.5814	-0.2030
C31		7.8000e-02	3.6527	-0.2700
H11		4.6000e-02	0.4000	0.4290
H21		3.5000e-02	2.3876	0.0900
H31		2.4000e-02	2.3876	0.0900
O11		1.9210e-01	3.1449	-0.6320
O21		1.2000e-01	3.0291	-0.5760

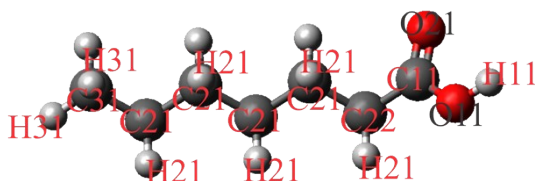


Table S16. Bond parameters of the heptanoic acid (CGENFF).

Bond type	$k_{r,ij} \left(\frac{kJ}{mol * \text{\AA}^2} \right)$	$r_{0,ij}(\text{\AA})$
C11-C22	200.0000	1.5220
C11-O11	230.0000	1.4000
C11-O21	750.0000	1.2200
C21-C21	222.5000	1.5300
C21-C22	222.5000	1.5300
C21-C31	222.5000	1.5280
C21-H21	309.0000	1.1110
C22-H21	309.0000	1.1110
C31-H31	322.0000	1.1110
H11-O11	545.0000	0.9600

Table S17. Angle parameters of the heptanoic acid (CGENFF).

Angle type	$k_{\theta,ijk} \left(\frac{kJ}{mol * rad^2} \right)$	$\theta_{0,ijk}(deg)$	$k_{UB,ik} \left(\frac{kJ}{mol * \text{\AA}^2} \right)$	$r_{0,ik}(\text{\AA})$
C11-C22-C21	52.0000	108.0000	0.0000	0.0000
C11-C22-H21	33.0000	109.5000	30.0000	2.1630
C11-O11-H11	55.0000	115.0000	0.0000	0.0000
C21-C21-C21	58.3500	113.6000	11.1600	2.5610
C21-C21-C22	58.3500	113.6000	11.1600	2.5610
C21-C21-C31	58.0000	115.0000	8.0000	2.5610
C21-C21-H21	26.5000	110.1000	22.5300	2.1790
C21-C22-H21	26.5000	110.1000	22.5300	2.1790
C21-C31-H31	34.6000	110.1000	22.5300	2.1790
C22-C11-O11	55.0000	110.5000	0.0000	0.0000
C22-C11-O21	70.0000	125.0000	20.0000	2.4420
C22-C21-H21	26.5000	110.1000	22.5300	2.1790

C31-C21-H21	34.6000	110.1000	22.5300	2.1790
H21-C21-H21	35.5000	109.0000	5.4000	1.8020
H21-C22-H21	35.5000	109.0000	5.4000	1.8020
H31-C31-H31	35.5000	108.4000	5.4000	1.8020
O11-C11-O21	50.0000	123.0000	210.0000	2.2620

Table S18. Dihedral proper parameters of the heptanoic acid (CGENFF).

Dihedral proper type	$k_{\phi,ijkl} \left(\frac{kJ}{mol} \right)$	$n(adi.)$	$\delta_{0,ijkl}(deg)$	Factorweight (adi.)
C21-C21-C21-C21	0.1497	3.0000	180.0000	1.0000
C21-C21-C21-C22	0.1497	3.0000	180.0000	1.0000
C21-C21-C21-C31	0.0813	3.0000	180.0000	1.0000
C21-C21-C21-H21	0.1950	3.0000	0.0000	1.0000
C21-C21-C22-C11	0.3500	3.0000	180.0000	1.0000
C21-C21-C22-H21	0.1950	3.0000	0.0000	1.0000
C21-C21-C31-H31	0.1600	3.0000	0.0000	1.0000
C22-C11-O11-H11	2.0500	2.0000	180.0000	1.0000
C22-C21-C21-H21	0.1950	3.0000	0.0000	1.0000
C31-C21-C21-H21	0.1800	3.0000	0.0000	1.0000
H21-C21-C21-H21	0.2200	3.0000	0.0000	1.0000
H21-C21-C22-C11	0.1950	3.0000	0.0000	1.0000
H21-C21-C22-H21	0.2200	3.0000	0.0000	1.0000
H21-C21-C31-H31	0.1600	3.0000	0.0000	1.0000
O11-C11-C22-C21	0.0000	6.0000	180.0000	1.0000
O11-C11-C22-H21	0.0000	6.0000	180.0000	1.0000
O21-C11-C22-C21	0.0500	6.0000	180.0000	1.0000
O21-C11-C22-H21	0.0000	6.0000	180.0000	1.0000
O21-C11-O11-H11	2.0500	2.0000	180.0000	1.0000

Table S19. Dihedral improper coefficients parameters of the heptanoic acid (CGENFF).

Dihedral improper type	$k_{\phi,ijk} \left(\frac{kJ}{mol * \text{\AA}^2} \right)$	$\phi_{0,ijkl}(\text{\AA}^2)$
C22-O11-C11-O21	65.0000	180.0000

Table S20. Lennard-Jones and partial charge parameters of the sodium heptanoate (CGENFF).

Atom type	Description	$\epsilon\left(\frac{kJ}{mol * \text{\AA}^2}\right)$	$\sigma(\text{\AA})$	$q(e)$
C11		7.0000e-02	3.5636	0.6220
C21		5.6000e-02	3.5814	-0.1800
C22		5.6000e-02	3.5814	-0.1790
C23		5.6000e-02	3.5814	-0.2830
C31		7.8000e-02	3.6527	-0.2700
H21		3.5000e-02	2.3876	0.0900
H31		2.4000e-02	2.3876	0.0900
O21		1.2000e-01	3.0291	-0.7600
Na		4.6900e-02	2.5137	1.0000

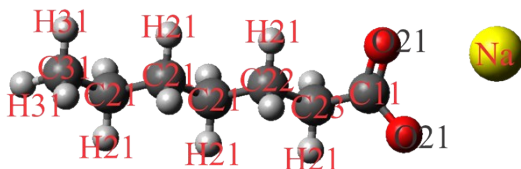


Table S21. Bond coefficients parameters of the sodium heptanoate (CGENFF).

Bond type	$k_{r,ij}\left(\frac{kJ}{mol * \text{\AA}^2}\right)$	$r_{0,ij}(\text{\AA})$
C11-C23	200.0000	1.5220
C11-O21	525.0000	1.2600
C21-C21	222.5000	1.5300
C21-C22	222.5000	1.5300
C21-C31	222.5000	1.5280
C21-H21	309.0000	1.1110
C22-C23	222.5000	1.5300
C22-H21	309.0000	1.1110
C23-H21	309.0000	1.1110
C31-H31	322.0000	1.1110

Table S22. Angle coefficients parameters of the sodium heptanoate (CGENFF).

Angle type	$k_{\theta,ijk}\left(\frac{kJ}{mol * rad^2}\right)$	$\theta_{0,ijk}(deg)$	$k_{UB,ik}\left(\frac{kJ}{mol * \text{\AA}^2}\right)$	$r_{0,ik}(\text{\AA})$
C11-C23-C22	52.0000	108.0000	0.0000	0.0000
C11-C23-H21	33.0000	109.5000	30.0000	2.1630
C21-C21-C21	58.3500	113.6000	11.1600	2.5610
C21-C21-C22	58.3500	113.6000	11.1600	2.5610
C21-C21-C31	58.0000	115.0000	8.0000	2.5610
C21-C21-H21	26.5000	110.1000	22.5300	2.1790
C21-C22-C23	58.3500	113.6000	11.1600	2.5610
C21-C22-H21	26.5000	110.1000	22.5300	2.1790
C21-C31-H31	34.6000	110.1000	22.5300	2.1790
C22-C21-H21	26.5000	110.1000	22.5300	2.1790
C22-C23-H21	26.5000	110.1000	22.5300	2.1790
C23-C11-O21	40.0000	116.0000	50.0000	2.3530

C23-C22-H21	26.5000	110.1000	22.5300	2.1790
C31-C21-H21	34.6000	110.1000	22.5300	2.1790
H21-C21-H21	35.5000	109.0000	5.4000	1.8020
H21-C22-H21	35.5000	109.0000	5.4000	1.8020
H21-C23-H21	35.5000	109.0000	5.4000	1.8020
H31-C31-H31	35.5000	108.4000	5.4000	1.8020
O21-C11-O21	100.0000	128.0000	70.0000	2.2587

Table S23. Dihedral proper coefficients parameters of the sodium heptanoate (CGENFF).

Dihedral proper type	$k_{\phi,ijkl} \left(\frac{kJ}{mol} \right)$	$n(adi.)$	$\delta_{0,ijkl}(deg)$	Factorweight (adi.)
C21-C21-C21-C22	0.1497	3.0000	180.0000	1.0000
C21-C21-C21-C31	0.0813	3.0000	180.0000	1.0000
C21-C21-C21-H21	0.1950	3.0000	0.0000	1.0000
C21-C21-C22-C23	0.1497	3.0000	180.0000	1.0000
C21-C21-C22-H21	0.1950	3.0000	0.0000	1.0000
C21-C21-C31-H31	0.1600	3.0000	0.0000	1.0000
C21-C22-C23-C11	0.1497	3.0000	180.0000	1.0000
C21-C22-C23-H21	0.1950	3.0000	0.0000	1.0000
C22-C21-C21-H21	0.1950	3.0000	0.0000	1.0000
C31-C21-C21-H21	0.1800	3.0000	0.0000	1.0000
H21-C21-C21-H21	0.2200	3.0000	0.0000	1.0000
H21-C21-C22-C23	0.1950	3.0000	0.0000	1.0000
H21-C21-C22-H21	0.2200	3.0000	0.0000	1.0000
H21-C21-C31-H31	0.1600	3.0000	0.0000	1.0000
H21-C22-C23-C11	0.1950	3.0000	0.0000	1.0000
H21-C22-C23-H21	0.2200	3.0000	0.0000	1.0000
O21-C11-C23-C22	0.0500	6.0000	180.0000	1.0000
O21-C11-C23-H21	0.0500	6.0000	180.0000	1.0000

Table S24. Dihedral improper coefficients parameters of the sodium heptanoate (CGENFF).

Dihedral improper type	$k_{\phi,ijk} \left(\frac{kJ}{mol * \text{\AA}^2} \right)$	$\phi_{0,ijkl}(\text{\AA}^2)$
C23-O21-C11-O21	96.0000	180.0000

Table S25. Lennard-Jones and partial charge parameters of the hexylamine (CGENFF).

Atom type	Description	$\epsilon \left(\frac{kJ}{mol * \text{\AA}^2} \right)$	$\sigma(\text{\AA})$	$q(e)$
C21		5.6000e-02	3.5814	-0.1800
C22		5.6000e-02	3.5814	-0.1850
C23		5.6000e-02	3.5814	0.0080
C31		7.8000e-02	3.6527	-0.2700
H11		1.0000e-02	1.5591	0.2960
H21		3.5000e-02	2.3876	0.0900
H31		2.4000e-02	2.3876	0.0900
N11		6.0000e-02	3.5458	-0.7750

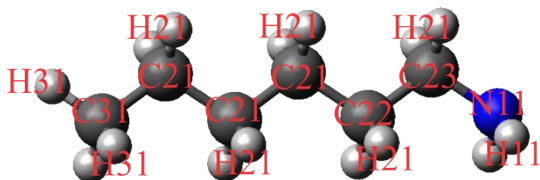


Table S26. Bond parameters of the hexylamine (CGENFF).

Bond type	$k_{r,ij} \left(\frac{kJ}{mol * \text{\AA}^2} \right)$	$r_{0,ij}(\text{\AA})$
C21-C21	222.5000	1.5300
C21-C22	222.5000	1.5300
C21-C31	222.5000	1.5280
C21-H21	309.0000	1.1110
C22-C23	222.5000	1.5300
C22-H21	309.0000	1.1110
C23-H21	309.0000	1.1110
C23-N11	263.0000	1.4740
C31-H31	322.0000	1.1110
H11-N11	453.1000	1.0140

Table S27. Angle parameters of the hexylamine (CGENFF).

Angle type	$k_{\theta,ijk} \left(\frac{kJ}{mol * rad^2} \right)$	$\theta_{0,ijk}(deg)$	$k_{UB,ik} \left(\frac{kJ}{mol * \text{\AA}^2} \right)$	$r_{0,ik}(\text{\AA})$
C21-C21-C21	58.3500	113.6000	11.1600	2.5610
C21-C21-C22	58.3500	113.6000	11.1600	2.5610
C21-C21-C31	58.0000	115.0000	8.0000	2.5610
C21-C21-H21	26.5000	110.1000	22.5300	2.1790
C21-C22-C23	58.3500	113.6000	11.1600	2.5610
C21-C22-H21	26.5000	110.1000	22.5300	2.1790
C21-C31-H31	34.6000	110.1000	22.5300	2.1790
C22-C21-H21	26.5000	110.1000	22.5300	2.1790
C22-C23-H21	26.5000	110.1000	22.5300	2.1790
C22-C23-N11	43.7000	112.2000	0.0000	0.0000
C23-C22-H21	26.5000	110.1000	22.5300	2.1790
C23-N11-H11	41.0000	112.1000	0.0000	0.0000
C31-C21-H21	34.6000	110.1000	22.5300	2.1790

H11-N11-H11	42.0000	105.8500	0.0000	0.0000
H21-C21-H21	35.5000	109.0000	5.4000	1.8020
H21-C22-H21	35.5000	109.0000	5.4000	1.8020
H21-C23-H21	35.5000	109.0000	5.4000	1.8020
H21-C23-N11	32.4000	109.5000	50.0000	2.1400
H31-C31-H31	35.5000	108.4000	5.4000	1.8020

Table S28. Dihedral proper parameters of the hexylamine (CGENFF).

Dihedral proper type	$k_{\varphi,ijkl} \left(\frac{kJ}{mol} \right)$	$n(adi.)$	$\delta_{0,ijkl}(deg)$	<i>Factorweight</i> (adi.)
C21-C21-C21-C22	0.1497	3.0000	180.0000	1.0000
C21-C21-C21-C31	0.0813	3.0000	180.0000	1.0000
C21-C21-C21-H21	0.1950	3.0000	0.0000	1.0000
C21-C21-C22-C23	0.1497	3.0000	180.0000	1.0000
C21-C21-C22-H21	0.1950	3.0000	0.0000	1.0000
C21-C21-C31-H31	0.1600	3.0000	0.0000	1.0000
C21-C22-C23-H21	0.1950	3.0000	0.0000	1.0000
C21-C22-C23-N11	0.3900	2.0000	0.0000	1.0000
C22-C21-C21-H21	0.1950	3.0000	0.0000	1.0000
C22-C23-N11-H11	0.1000	3.0000	0.0000	1.0000
C31-C21-C21-H21	0.1800	3.0000	0.0000	1.0000
H21-C21-C21-H21	0.2200	3.0000	0.0000	1.0000
H21-C21-C22-C23	0.1950	3.0000	0.0000	1.0000
H21-C21-C22-H21	0.2200	3.0000	0.0000	1.0000
H21-C21-C31-H31	0.1600	3.0000	0.0000	1.0000
H21-C22-C23-H21	0.2200	3.0000	0.0000	1.0000
H21-C22-C23-N11	0.1600	3.0000	0.0000	1.0000
H21-C23-N11-H11	0.0100	3.0000	0.0000	1.0000

Table S29. Lennard-Jones and partial charge parameters of the chlorine hexylammonium (CGENFF).

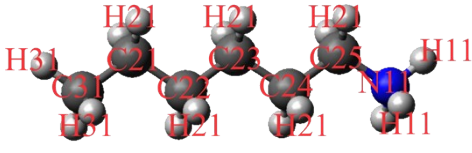

Atom type	Description	$\epsilon \left(\frac{kJ}{mol * \text{\AA}^2} \right)$	$\sigma (\text{\AA})$	$q(e)$
C21		5.6000e-02	3.5814	-0.1800
C22		5.6000e-02	3.5814	-0.1810
C23		5.6000e-02	3.5814	-0.1390
C24		5.6000e-02	3.5814	-0.2140
C25		5.5000e-02	3.8754	0.1250
C31		7.8000e-02	3.6527	-0.2700
H11		4.6000e-02	0.4000	0.3300
H21		3.5000e-02	2.3876	0.0900
H31		2.4000e-02	2.3876	0.0900
N1		2.0000e-01	3.2963	-0.3010
Cl		1.5000e-01	4.0445	-1.0000

Table S30. Bond parameters of the chlorine hexylammonium (CGENFF).

Bond type	$k_{r,ij} \left(\frac{kJ}{mol * \text{\AA}^2} \right)$	$r_{0,ij} (\text{\AA})$
C21-C22	222.5000	1.5300
C21-C31	222.5000	1.5280
C21-H21	309.0000	1.1110
C22-C23	222.5000	1.5300
C22-H21	309.0000	1.1110
C23-C24	222.5000	1.5300
C23-H21	309.0000	1.1110
C24-C25	222.5000	1.5300
C24-H21	309.0000	1.1110
C25-H21	284.5000	1.1000
C25-N1	200.0000	1.4900
C31-H31	322.0000	1.1110
H11-N1	403.0000	1.0400

Table S31. Angle parameters of the chlorine hexylammonium (CGENFF).

Angle type	$k_{\theta,ijk} \left(\frac{kJ}{mol * rad^2} \right)$	$\theta_{0,ijk} (deg)$	$k_{UB,ik} \left(\frac{kJ}{mol * \text{\AA}^2} \right)$	$r_{0,ik} (\text{\AA})$
C21-C22-C23	58.3500	113.6000	11.1600	2.5610
C21-C22-H21	26.5000	110.1000	22.5300	2.1790
C21-C31-H31	34.6000	110.1000	22.5300	2.1790
C22-C21-C31	58.0000	115.0000	8.0000	2.5610
C22-C21-H21	26.5000	110.1000	22.5300	2.1790
C22-C23-C24	58.3500	113.6000	11.1600	2.5610
C22-C23-H21	26.5000	110.1000	22.5300	2.1790

C23-C22-H21	26.5000	110.1000	22.5300	2.1790
C23-C24-C25	58.3500	110.5000	11.1600	2.5610
C23-C24-H21	26.5000	110.1000	22.5300	2.1790
C24-C23-H21	26.5000	110.1000	22.5300	2.1790
C24-C25-H21	26.5000	111.8000	22.5300	2.1790
C24-C25-N1	67.7000	110.0000	0.0000	0.0000
C25-C24-H21	26.5000	110.1000	22.5300	2.1790
C25-N1-H11	30.0000	109.5000	20.0000	2.0740
C31-C21-H21	34.6000	110.1000	22.5300	2.1790
H11-N1-H11	44.0000	109.5000	0.0000	0.0000
H21-C21-H21	35.5000	109.0000	5.4000	1.8020
H21-C22-H21	35.5000	109.0000	5.4000	1.8020
H21-C23-H21	35.5000	109.0000	5.4000	1.8020
H21-C24-H21	35.5000	109.0000	5.4000	1.8020
H21-C25-H21	35.5000	109.0000	5.4000	1.8020
H21-C25-N1	45.0000	107.5000	35.0000	2.1010
H31-C31-H31	35.5000	108.4000	5.4000	1.8020

Table S32. Dihedral proper parameters of the chlorine hexylammonium (CGENFF).

Dihedral proper type	$k_{\phi,ijkl} \left(\frac{kJ}{mol} \right)$	$n(adi.)$	$\delta_{0,ijkl}(deg)$	Factorweight (adi.)
C21-C22-C23-C24	0.1497	3.0000	180.0000	1.0000
C21-C22-C23-H21	0.1950	3.0000	0.0000	1.0000
C22-C21-C31-H31	0.1600	3.0000	0.0000	1.0000
C22-C23-C24-C25	0.1950	3.0000	0.0000	1.0000
C22-C23-C24-H21	0.1950	3.0000	0.0000	1.0000
C23-C24-C25-H21	0.1950	3.0000	0.0000	1.0000
C23-C24-C25-N1	0.1950	3.0000	0.0000	1.0000
C24-C25-N1-H11	0.1000	3.0000	0.0000	1.0000
C31-C21-C22-C23	0.0813	3.0000	180.0000	1.0000
C31-C21-C22-H21	0.1800	3.0000	0.0000	1.0000
H21-C21-C22-C23	0.1950	3.0000	0.0000	1.0000
H21-C21-C22-H21	0.2200	3.0000	0.0000	1.0000
H21-C21-C31-H31	0.1600	3.0000	0.0000	1.0000
H21-C22-C23-C24	0.1950	3.0000	0.0000	1.0000
H21-C22-C23-H21	0.2200	3.0000	0.0000	1.0000
H21-C23-C24-C25	0.1950	3.0000	0.0000	1.0000
H21-C23-C24-H21	0.2200	3.0000	0.0000	1.0000
H21-C24-C25-H21	0.1950	3.0000	0.0000	1.0000
H21-C24-C25-N1	0.1950	3.0000	0.0000	1.0000
H21-C25-N1-H11	0.1000	3.0000	0.0000	1.0000

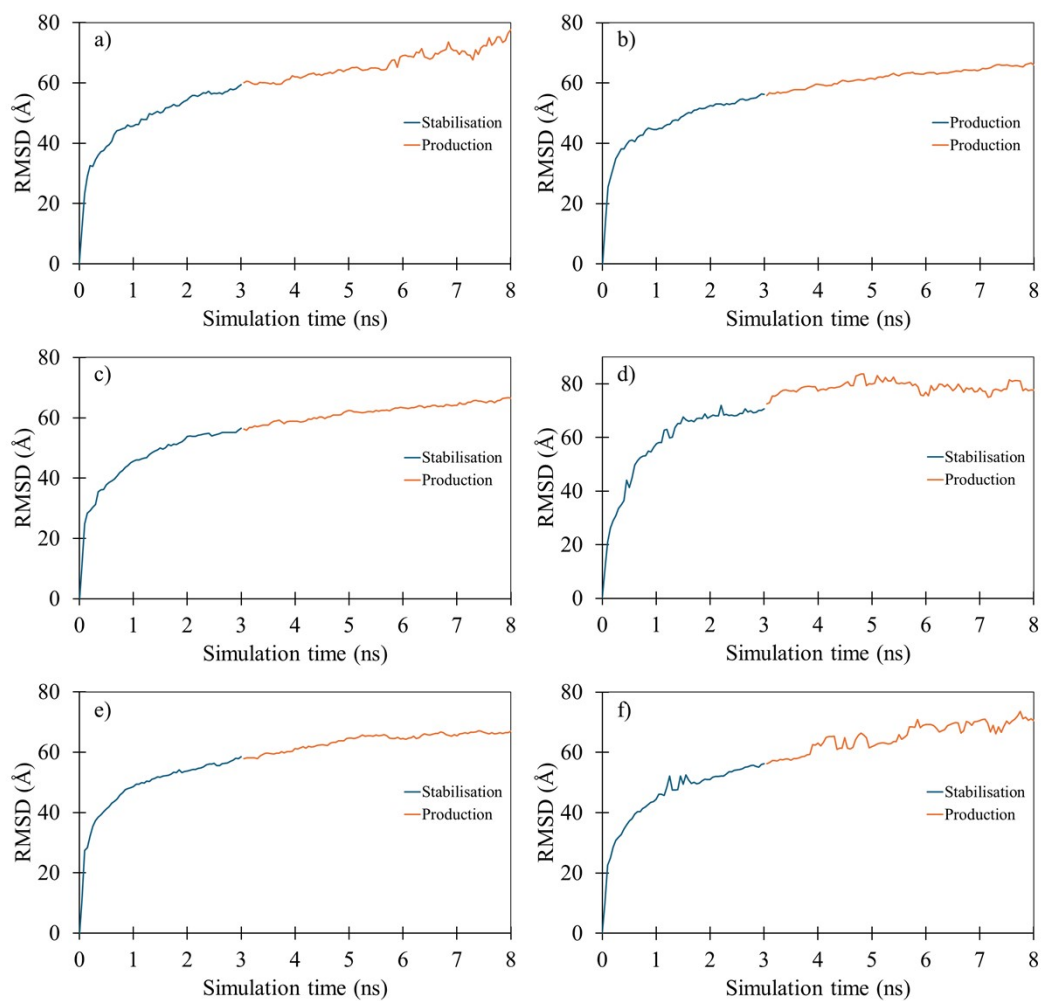


Figure S1. Mean-squared displacement (MSD) for direct emulsions on the basal surface of illite. a) the aromatic crude oil model in water system. b) the aliphatic crude oil model in water system. c) the polar A crude oil model in water at $\text{pH} \ll 4.4$ system. d) the polar A crude oil model in water at $\text{pH} \gg 4.4$ system. e) the polar B crude oil model in water at $\text{pH} \gg 10.64$ system. f) the polar B crude oil model in water at $\text{pH} \ll 10.64$ system.

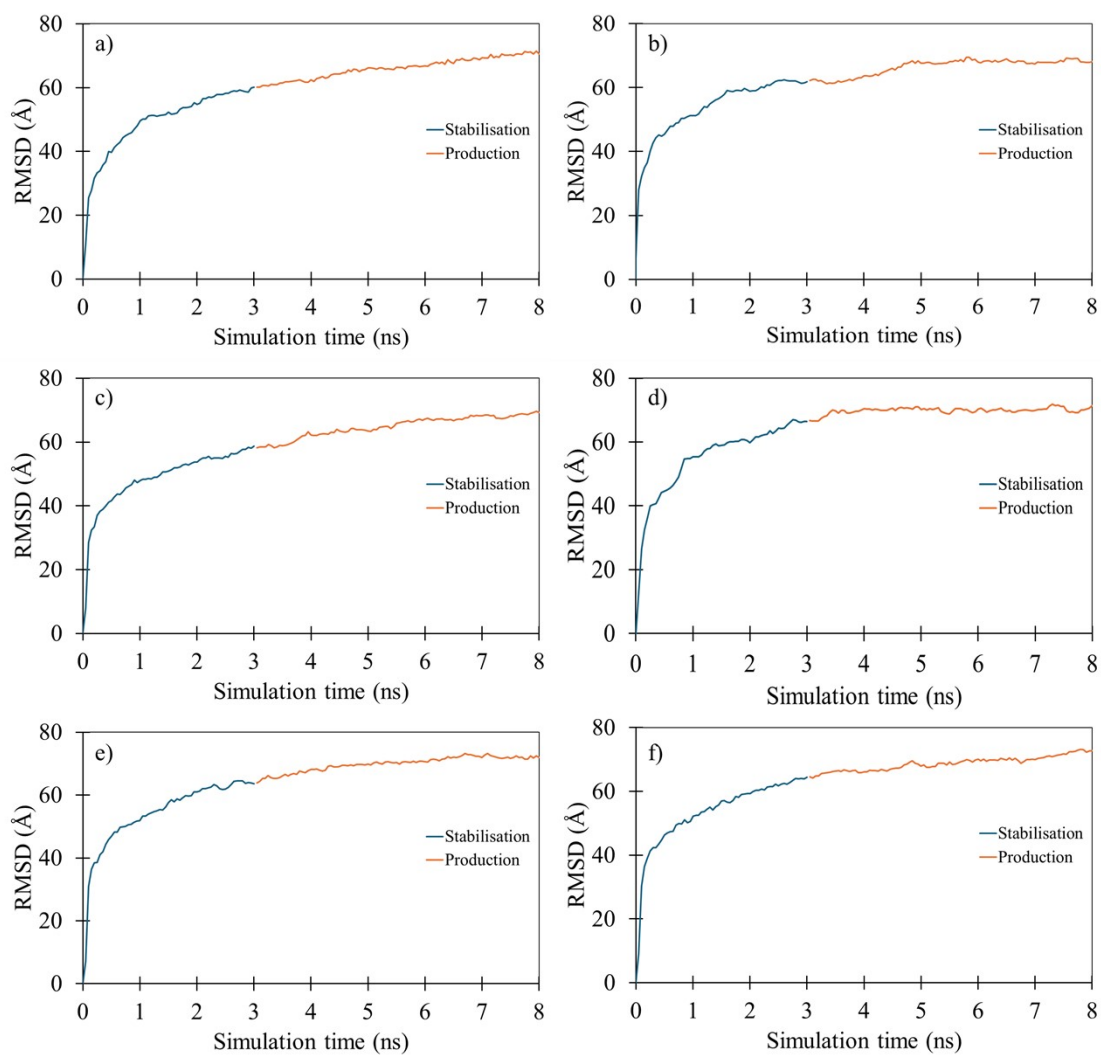


Figure S2. Mean-squared displacement (MSD) for indirect emulsions on the basal surface of illite. a) Water in the aromatic crude oil model system. b) Water in the aliphatic crude oil model in water system. c) Water at $\text{pH} \ll 4.4$ in the polar A crude oil model. d) Water at $\text{pH} \gg 10.64$ in the polar A crude oil model system. e) Water at $\text{pH} \ll 10.64$ in the polar B crude oil model system.

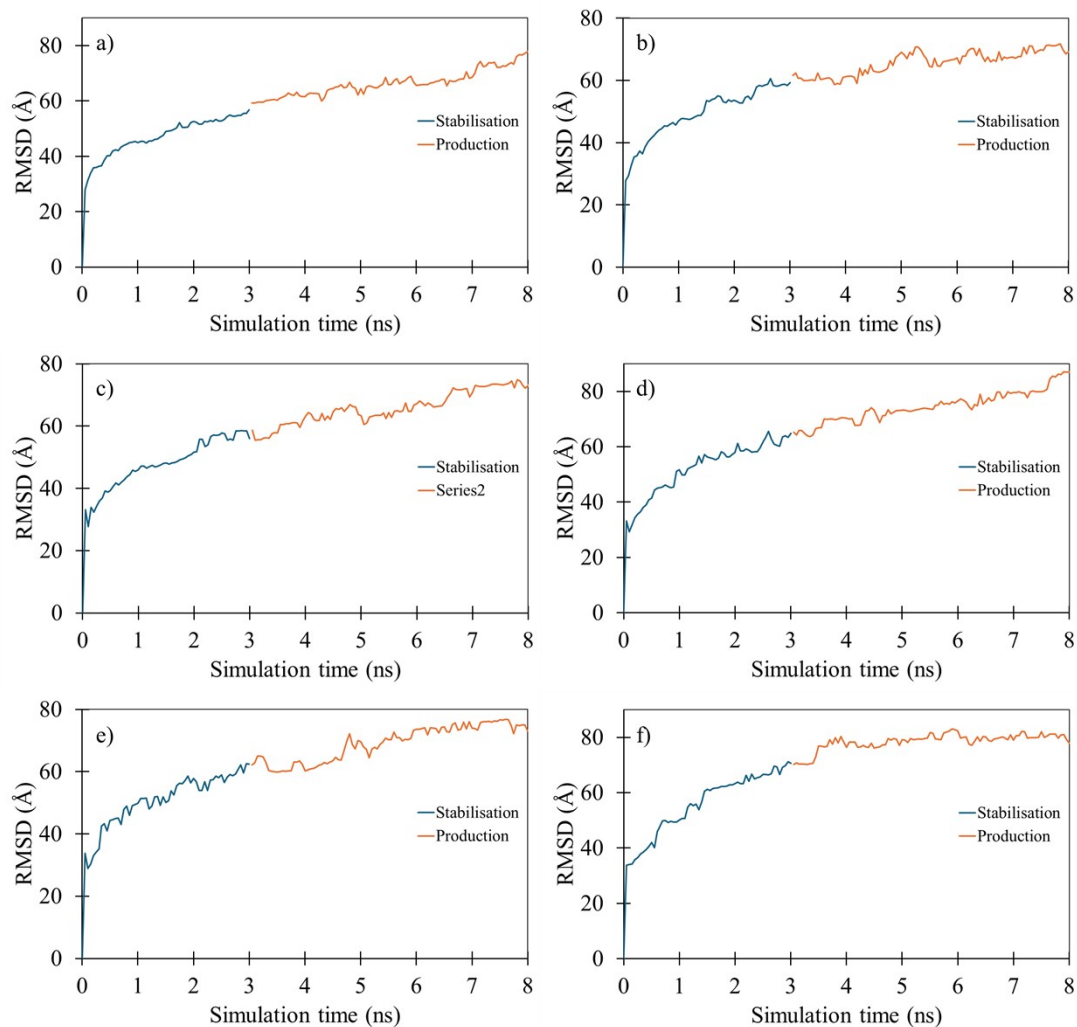


Figure S3. Mean-squared displacement (MSD) for direct emulsions on the edge surface of illite. a) the aromatic crude oil model in water system. b) the aliphatic crude oil model in water system. c) the polar A crude oil model in water at $\text{pH} \ll 4.4$ system. d) the polar A crude oil model in water at $\text{pH} \gg 4.4$ system. e) the polar B crude oil model in water at $\text{pH} \gg 10.64$ system. f) the polar B crude oil model in water at $\text{pH} \ll 10.64$ system.

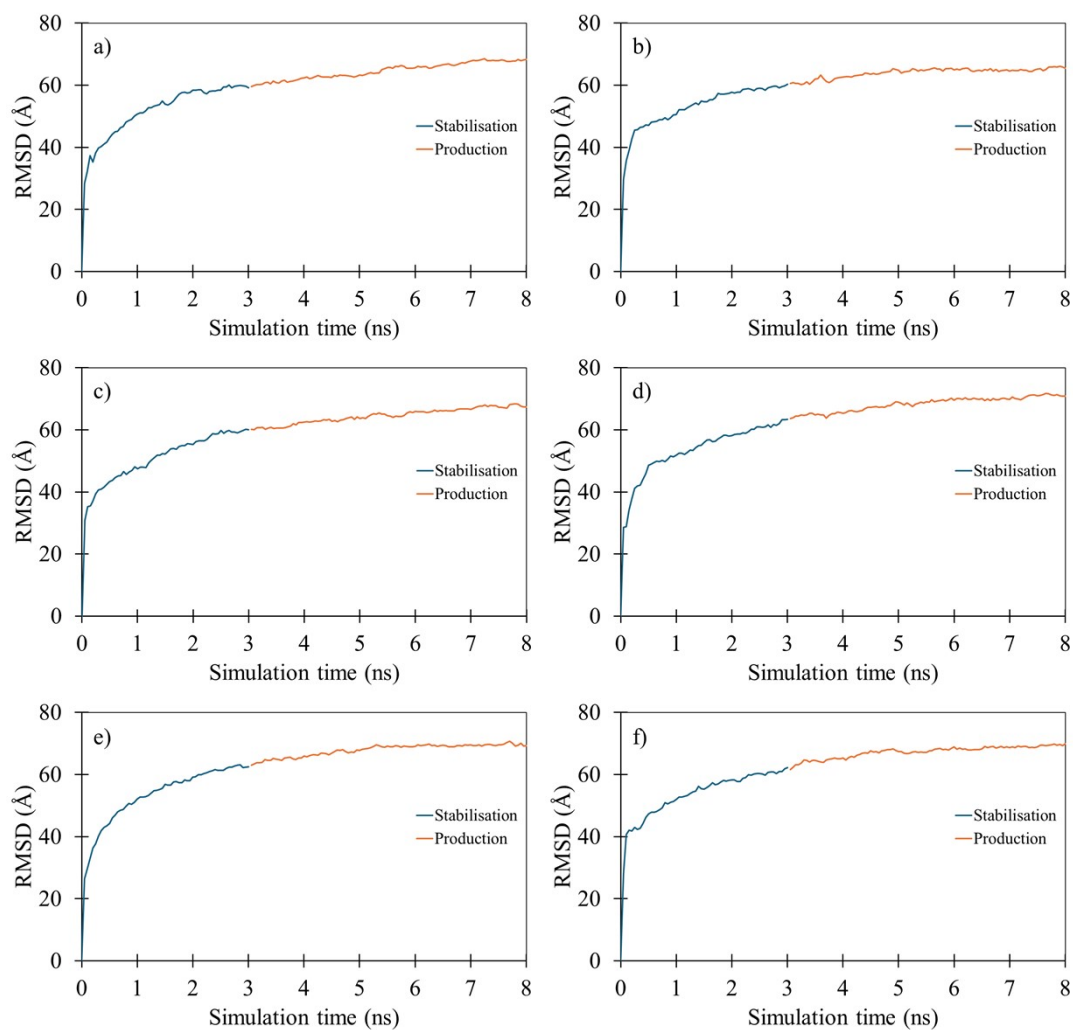


Figure S4. Mean-squared displacement (MSD) for indirect emulsions on the edge surface of illite. a) Water in the aromatic crude oil model system. b) Water in the aliphatic crude oil model in water system. c) Water at $\text{pH} \ll 4.4$ in the polar A crude oil model. d) Water at $\text{pH} \gg 10.64$ in the polar A crude oil model system. e) Water at $\text{pH} \ll 10.64$ in the polar B crude oil model system.

Final configurations and density profiles for each simulation of inverse emulsion on the basal surface (001). Crude oil models are: toluene (aromatic), heptane (aliphatic), heptane – heptanoic acid (polar A), heptane – hexylamine (polar B).

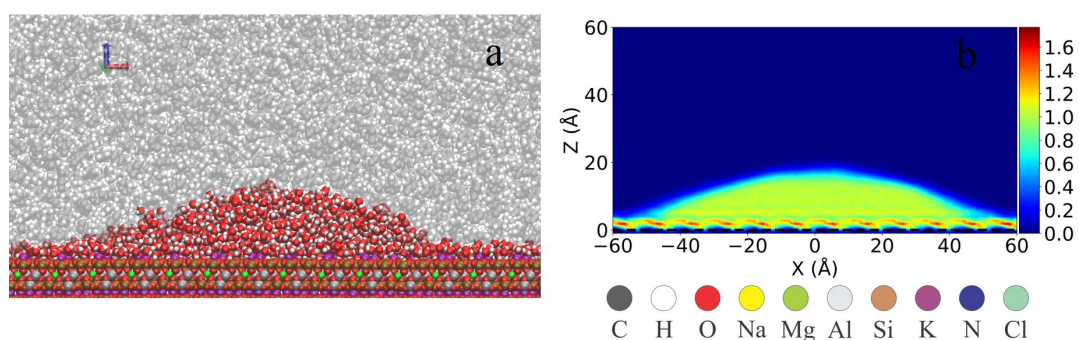


Figure S5. a) Screenshot at 8 ns of the simulation of the water in aromatic crude oil model on the basal surface. b) Corresponding density profile captured at the production stage.

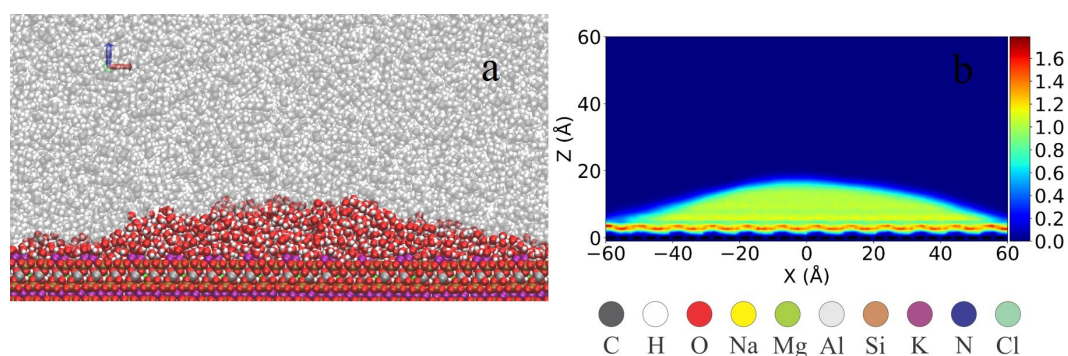


Figure S6. a) Screenshot at 8 ns of the simulation of the water in aliphatic crude oil model on the basal surface. b) Corresponding density profile captured at the production stage.

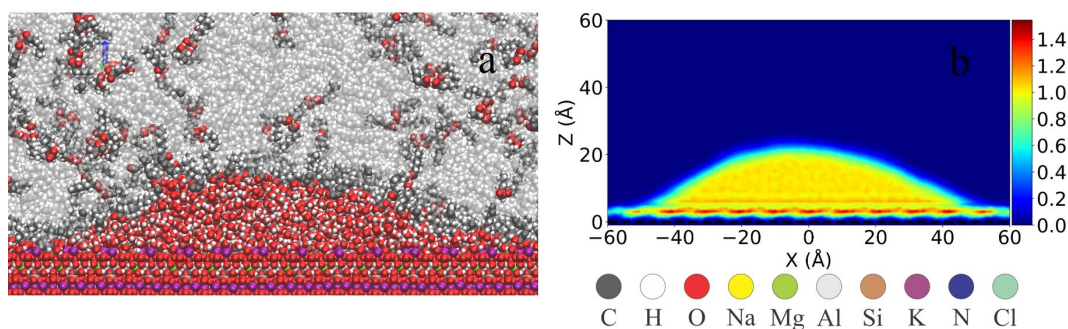


Figure S7. a) Screenshot at 8 ns of the simulation of the water at pH << 4.4 in polar A crude oil model on the basal surface. b) Corresponding density profile captured at the production stage.

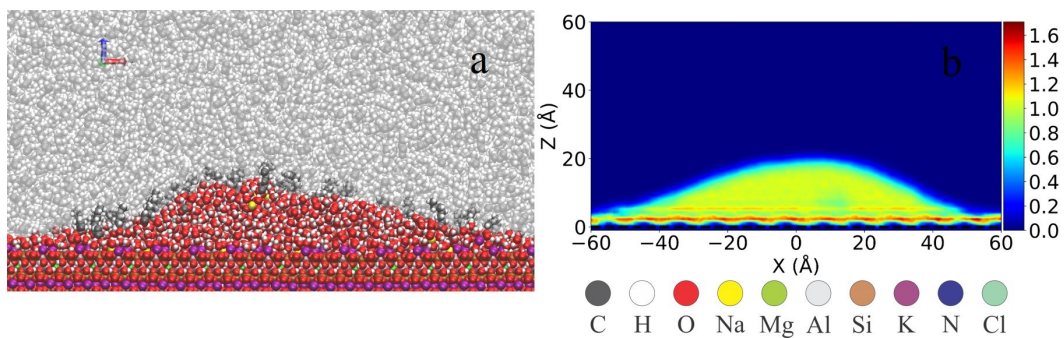


Figure S8. a) Screenshot at 8 ns of the simulation of the water at $\text{pH} \gg 4.4$ in polar A crude oil model on the basal surface. b) Corresponding density profile captured at the production.

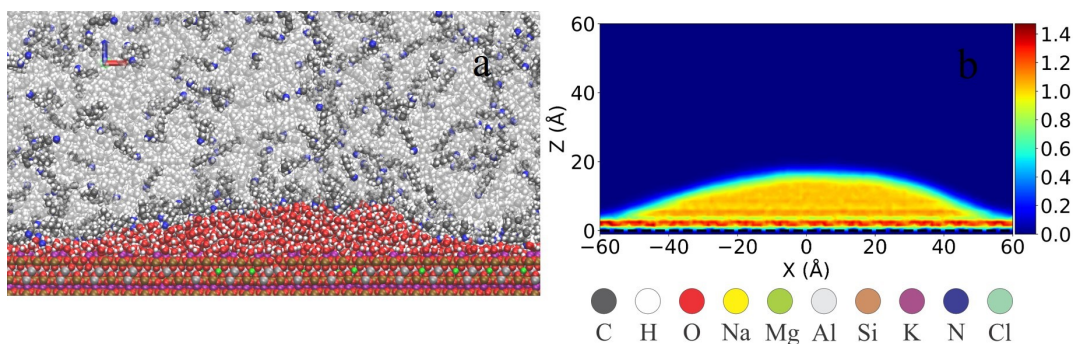


Figure S9. a) Screenshot at 8 ns of the simulation of the water at $\text{pH} \gg 10.64$ in polar B crude oil model on the basal surface. b) Corresponding density profile captured at the production stage.

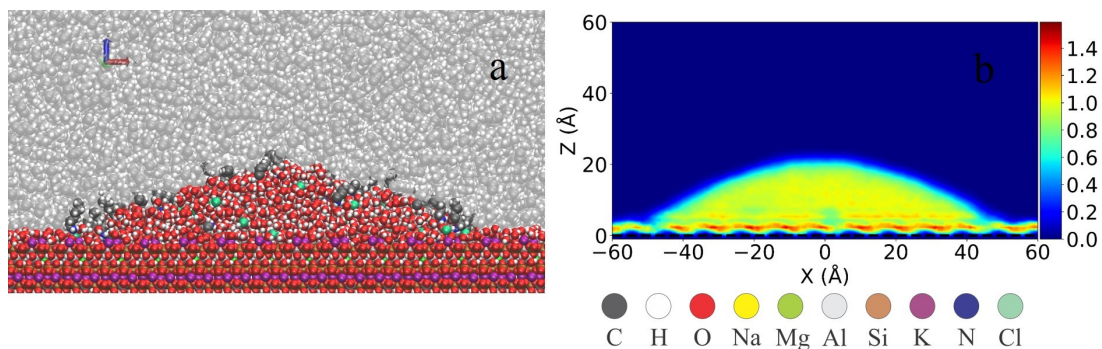


Figure S10. a) Screenshot at 8 ns of the simulation of the water at $\text{pH} \ll 10.64$ in polar B crude oil model on the basal surface. b) Corresponding density profile captured at the production stage.

Final configurations and density profiles for each simulation of direct emulsions on the basal surface (001). Crude oil models are: toluene (aromatic), heptane (aliphatic), heptane – heptanoic acid (polar A), heptane – hexylamine (polar B).

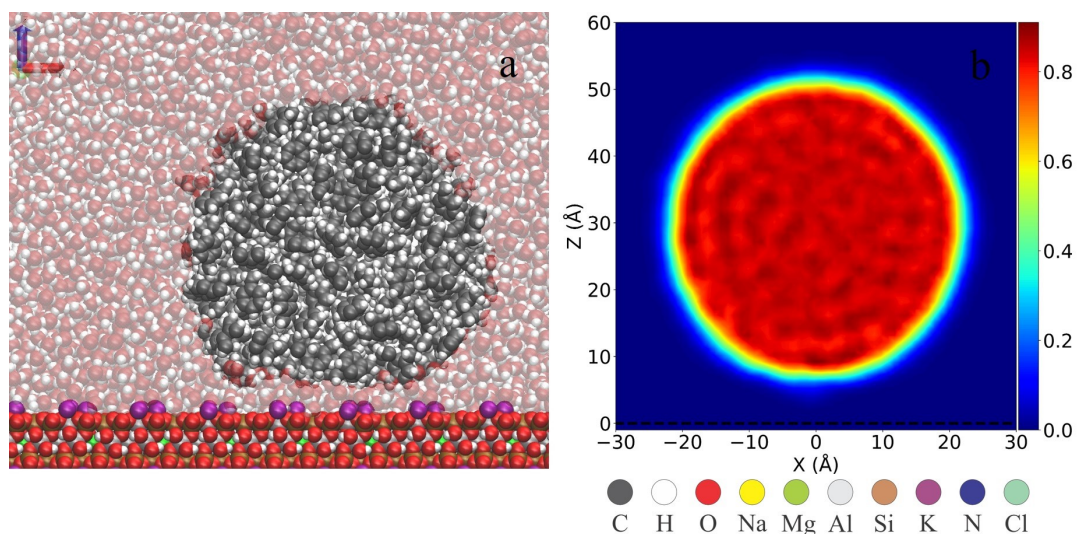


Figure S11. a) Screenshot at 8 ns of the simulation of the aromatic crude oil model in water on the basal surface. b) Corresponding density profile captured at the production stage.

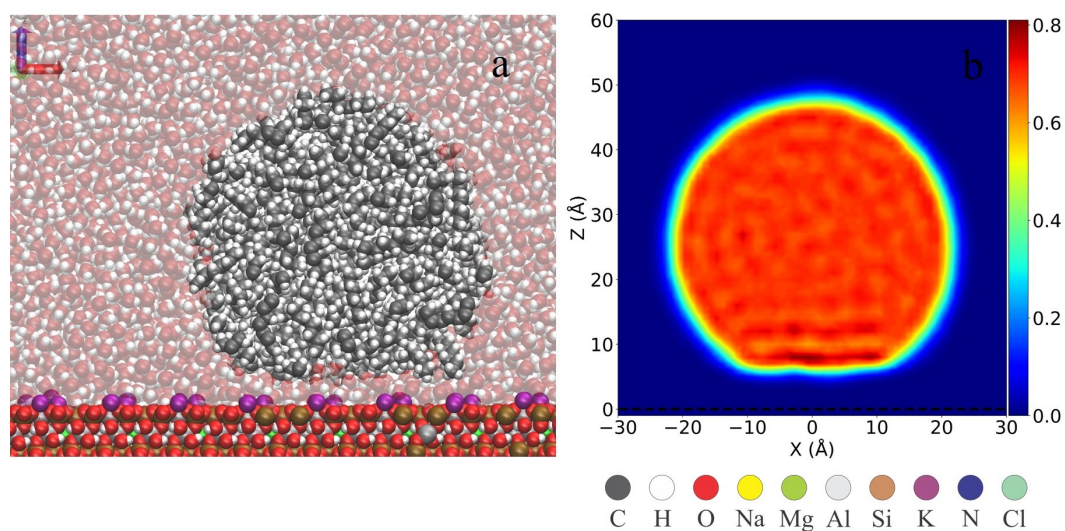


Figure S12. a) Screenshot at 8 ns of the simulation of the aliphatic crude oil model in water on the basal surface. b) Corresponding density profile captured at the production stage.

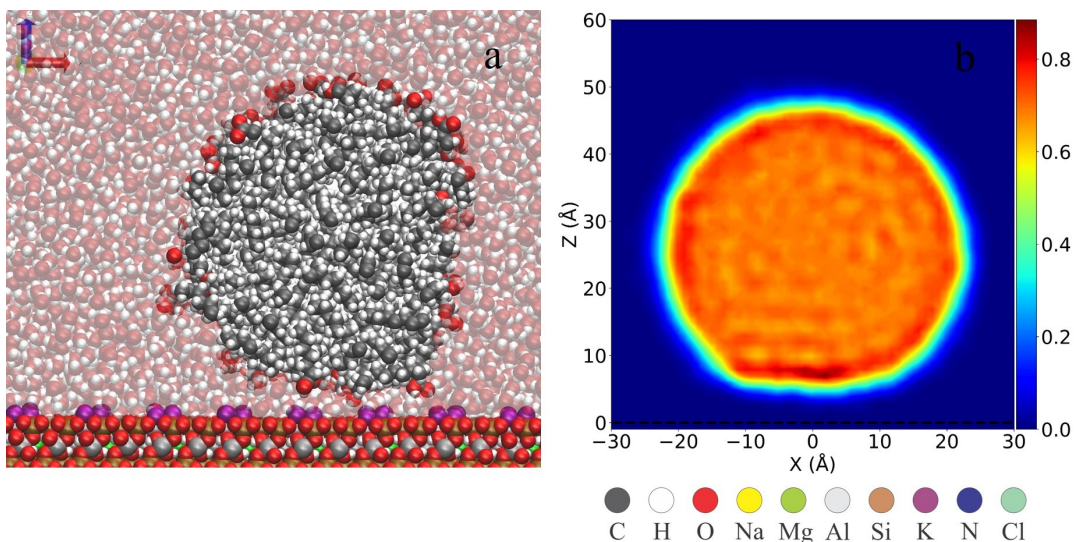


Figure S13. a) Screenshot at 8 ns of the simulation of the polar A crude oil model in water at $\text{pH} \ll 4.4$ on the basal surface. b) Corresponding density profile captured at the production stage.

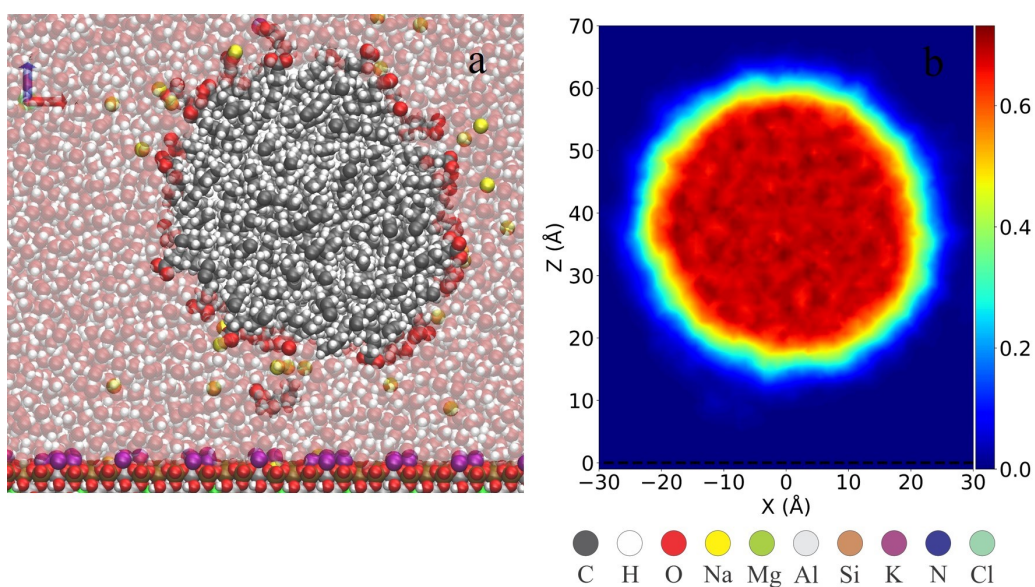


Figure S14. Screenshot at 8 ns of the simulation of the polar A crude oil model in water at $\text{pH} \gg 4.4$ on the basal surface. b) Corresponding density profile captured at the production stage.

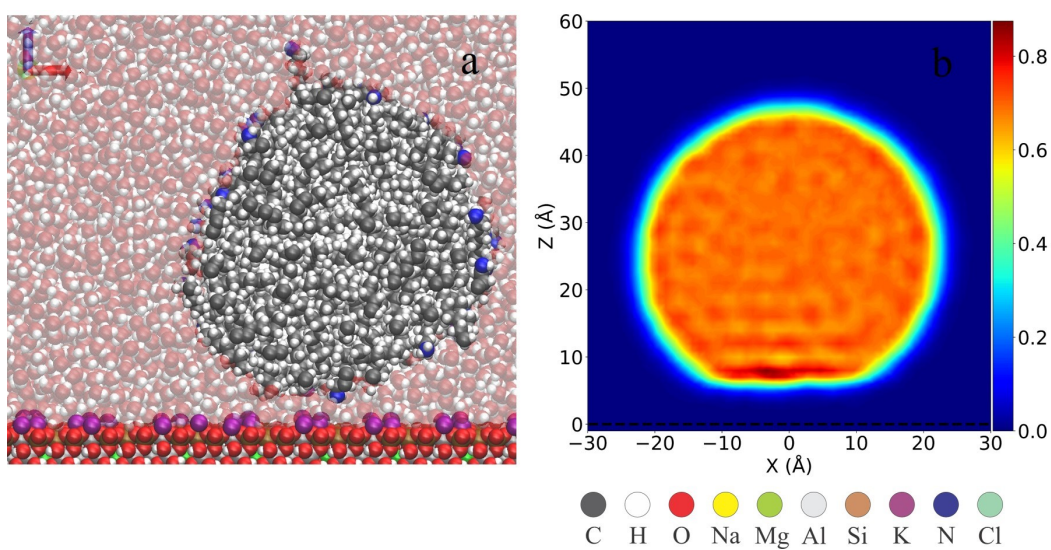


Figure S15. a) Screenshot at 8 ns of the simulation of the polar B crude oil model in water at $\text{pH} \gg 10.64$ on the basal surface. b) Corresponding density profile captured at the production stage.

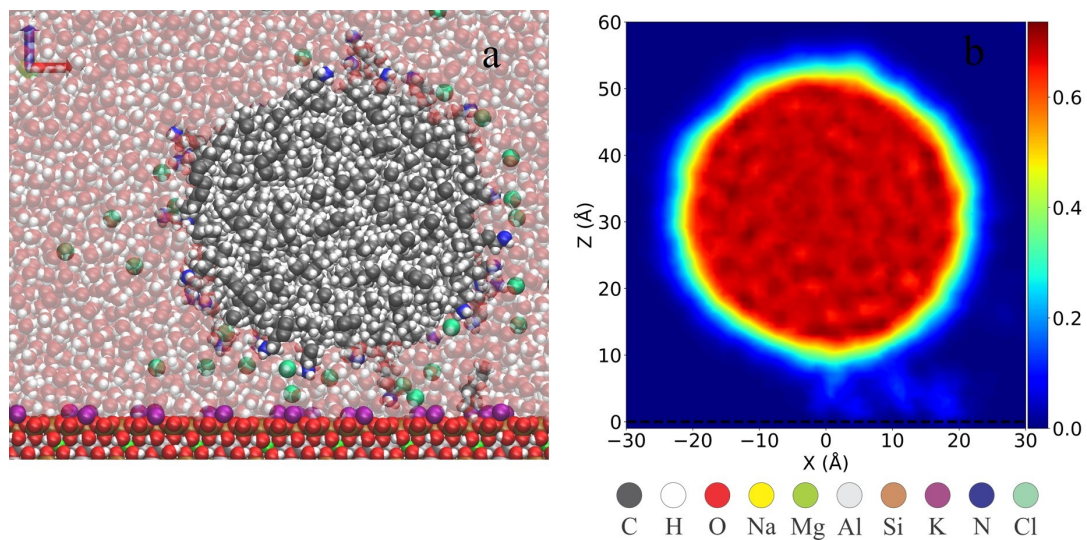


Figure S16. a) Screenshot at 8 ns of the simulation of the polar B crude oil model in water at $\text{pH} \ll 10.64$ on the basal surface. b) Corresponding density profile captured at the production stage.

Final configurations and density profiles for each simulation of inverse emulsions on the edge surface (010). Crude oil models are: toluene (aromatic), heptane (aliphatic), heptane – heptanoic acid (polar A), heptane – hexylamine (polar B).

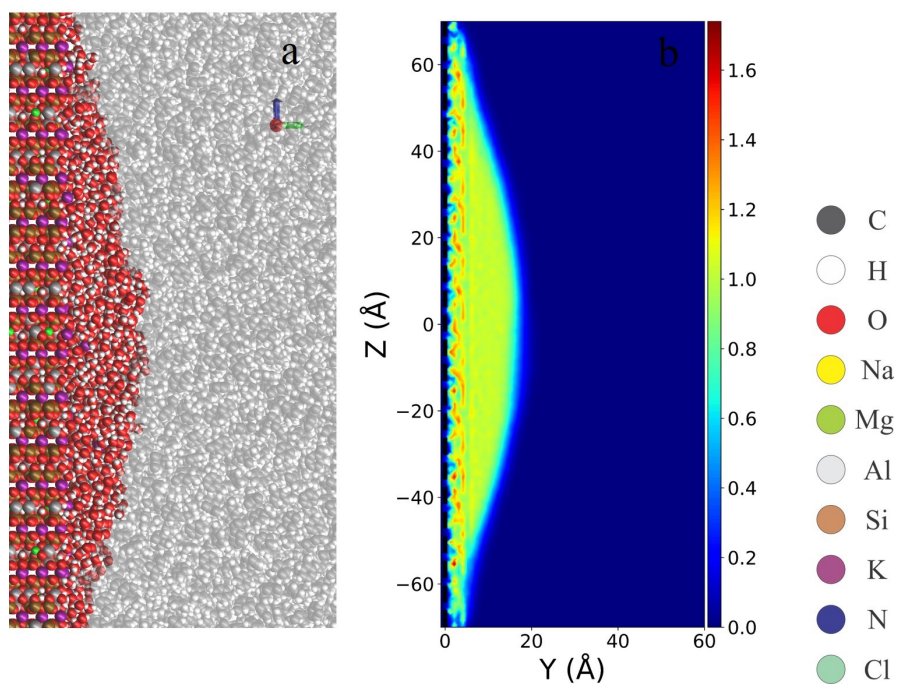


Figure S17. a) Screenshot at 8 ns of the simulation of the water in aromatic crude oil model on the edge surface. b) Corresponding density profile captured at the production stage.

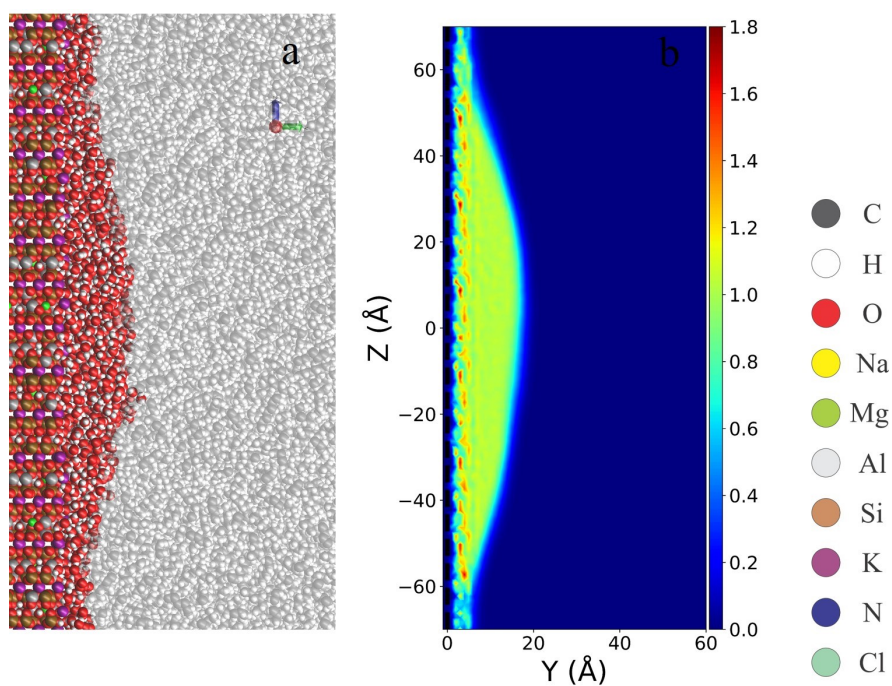


Figure S18. a) Screenshot at 8 ns of the simulation of the water in aliphatic crude oil model on the edge surface. b) Corresponding density profile captured at the production stage.

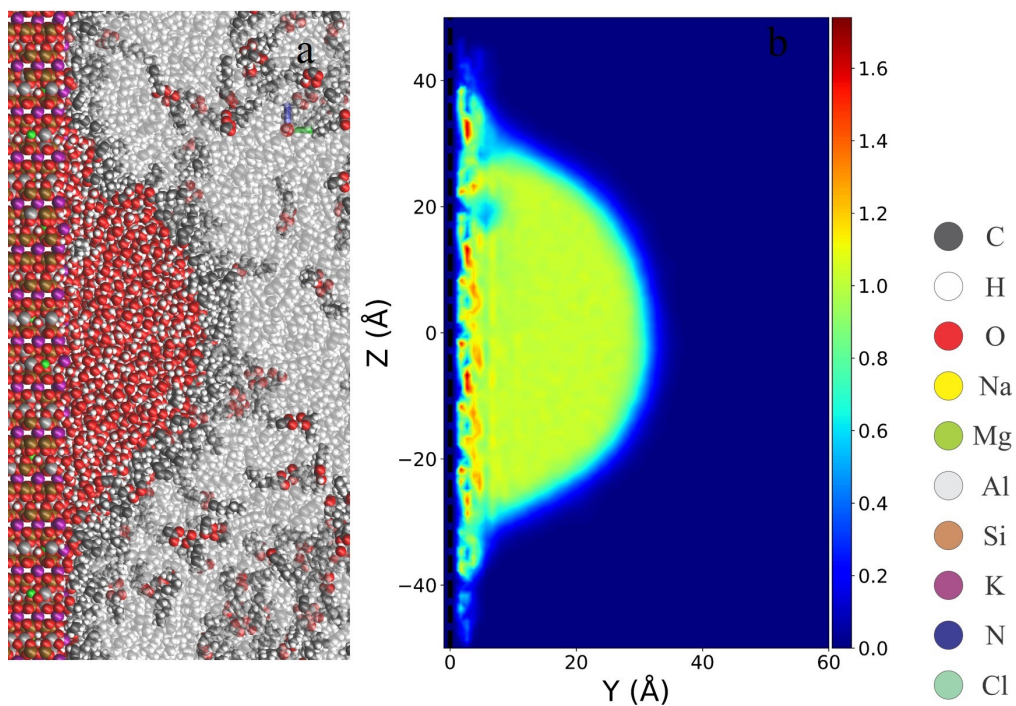


Figure S19. a) Screenshot at 8 ns of the simulation of the water at $\text{pH} \ll 4.4$ in polar A crude oil model on the edge surface. b) Corresponding density profile captured at the production stage.

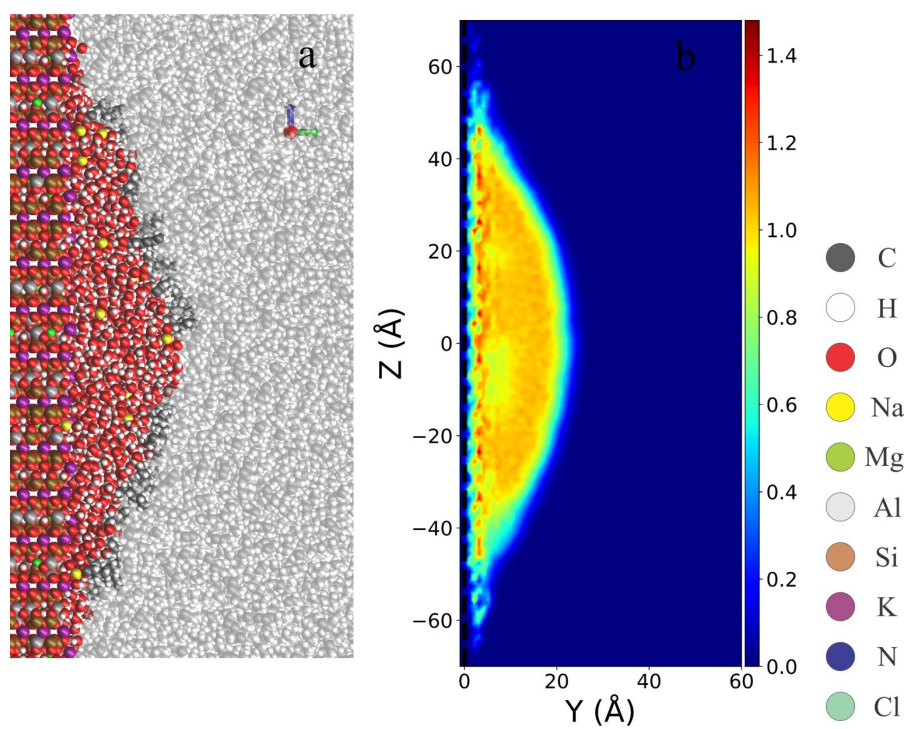


Figure S20. a) Screenshot at 8 ns of the simulation of the water at $\text{pH} \gg 4.4$ in polar A crude oil model on the edge surface. b) Corresponding density profile captured at the production stage.

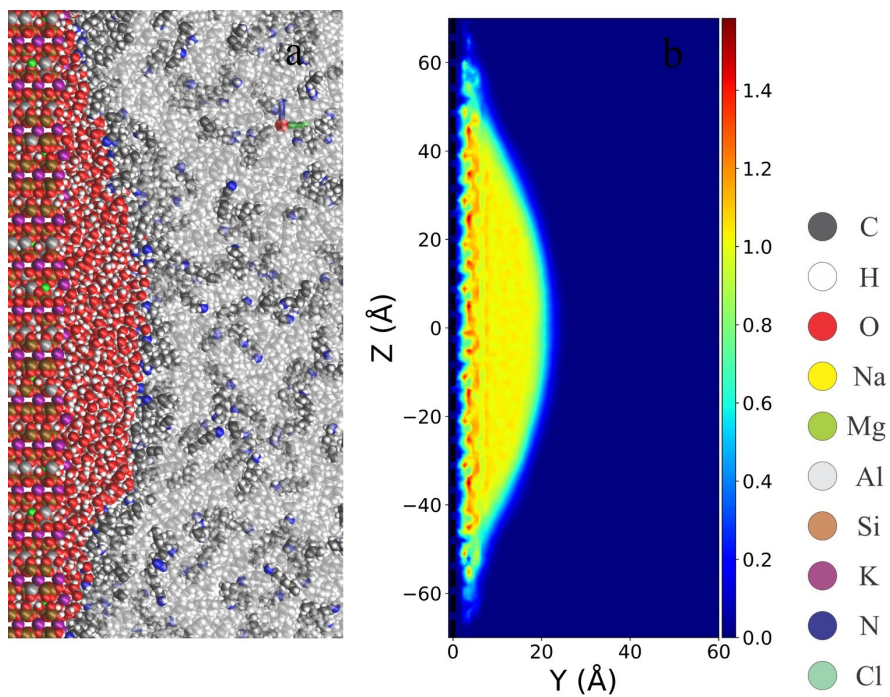


Figure S21. a) Screenshot at 8 ns of the simulation of the water at $\text{pH} \gg 10.64$ in polar B crude oil model on the edge surface. b) Corresponding density profile captured at the production stage.

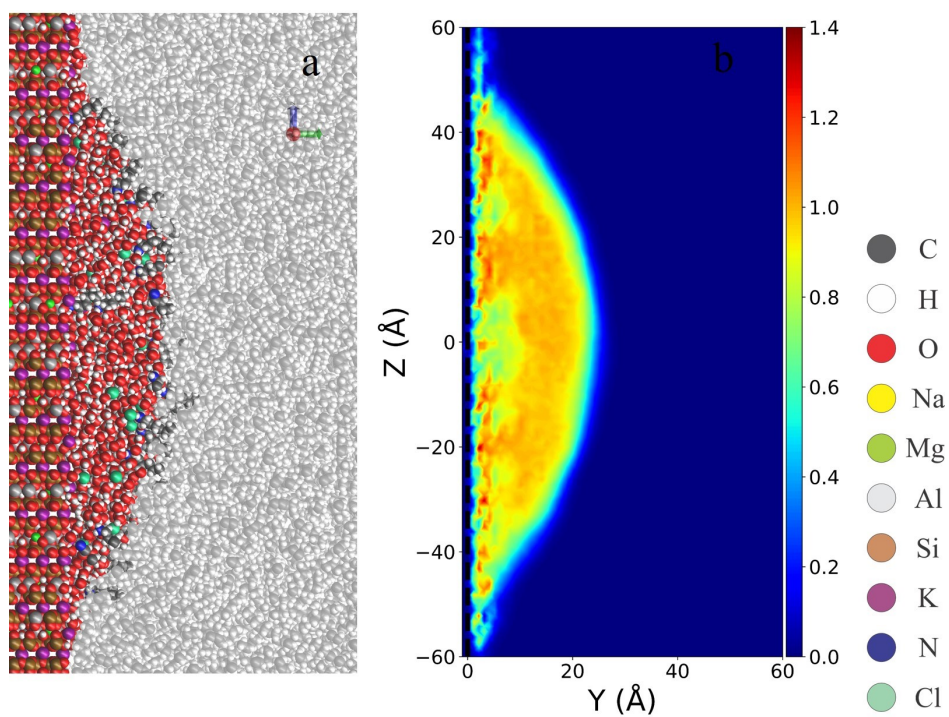


Figure S22. a) Screenshot at 8 ns of the simulation of the water at $\text{pH} \ll 10.64$ in polar B crude oil model on the edge surface. b) Corresponding density profile captured at the production stage.

Final configurations and density profiles for each simulation of direct emulsions on the edge surface (010). Crude oil models are: toluene (aromatic), heptane (aliphatic), heptane – heptanoic acid (polar A), heptane – hexylamine (polar B).

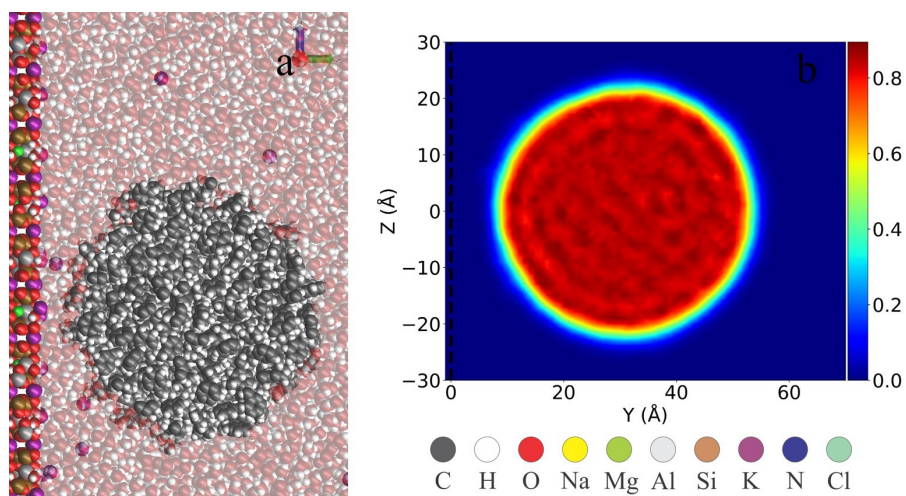


Figure S23. a) Screenshot at 8 ns of the simulation of the aromatic crude oil model in water on the edge surface. b) Corresponding density profile captured at the production stage.

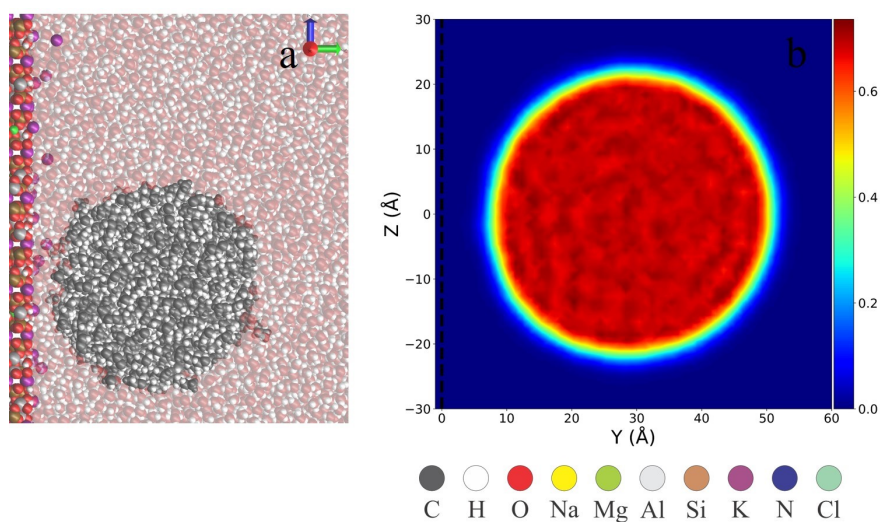


Figure S24. a) Screenshot at 8 ns of the simulation of the aliphatic crude oil model in water on the edge surface. b) Corresponding density profile captured at the production stage.

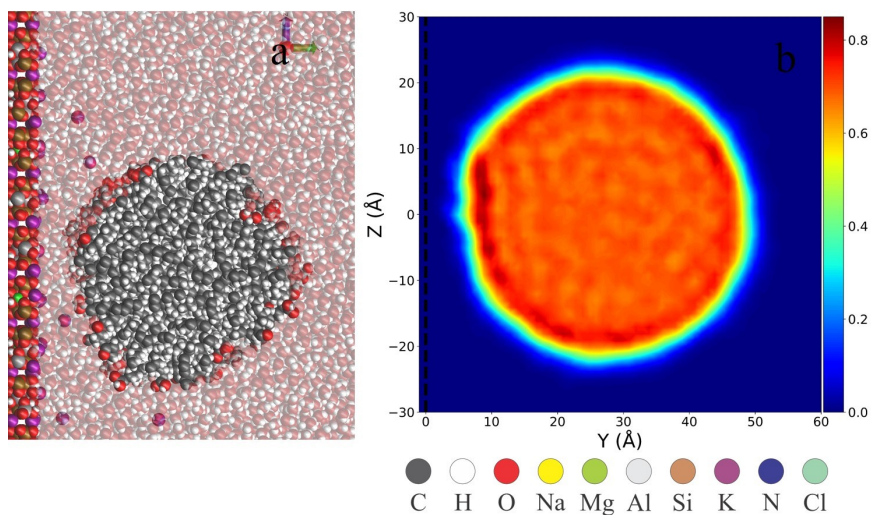


Figure S25. a) Screenshot at 8 ns of the simulation of the polar A crude oil model in water at $\text{pH} \ll 4.4$ on the edge surface. b) Corresponding density profile captured at the production stage.

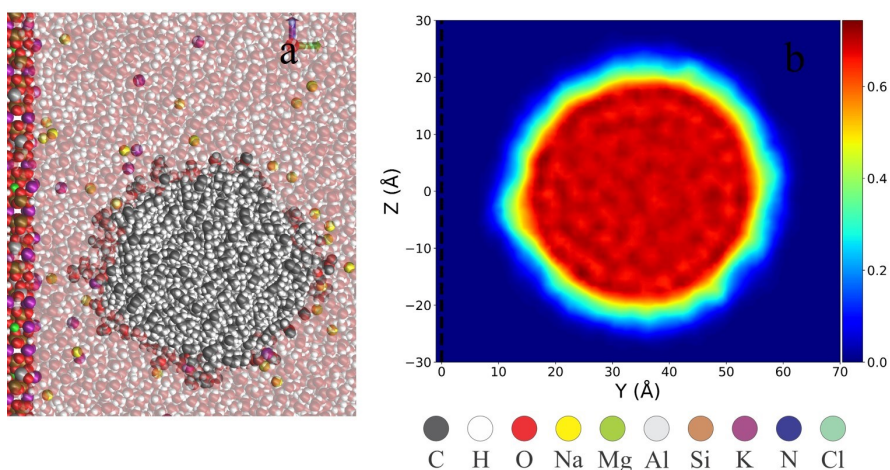


Figure S26. Screenshot at 8 ns of the simulation of the polar A crude oil model in water at $\text{pH} \gg 4.4$ on the edge surface. b) Corresponding density profile captured at the production stage.

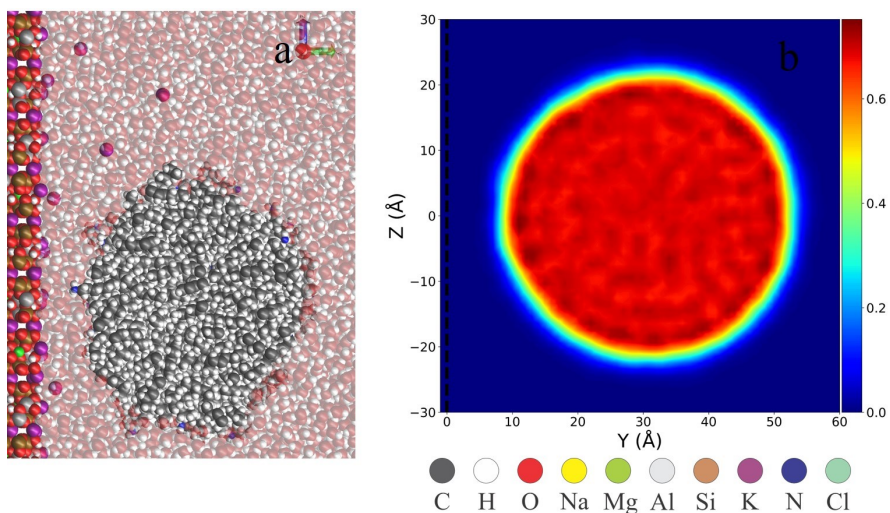


Figure S27. a) Screenshot at 8 ns of the simulation of the polar B crude oil model in water at $\text{pH} \gg 10.64$ on the edge surface. b) Corresponding density profile captured at the production stage.

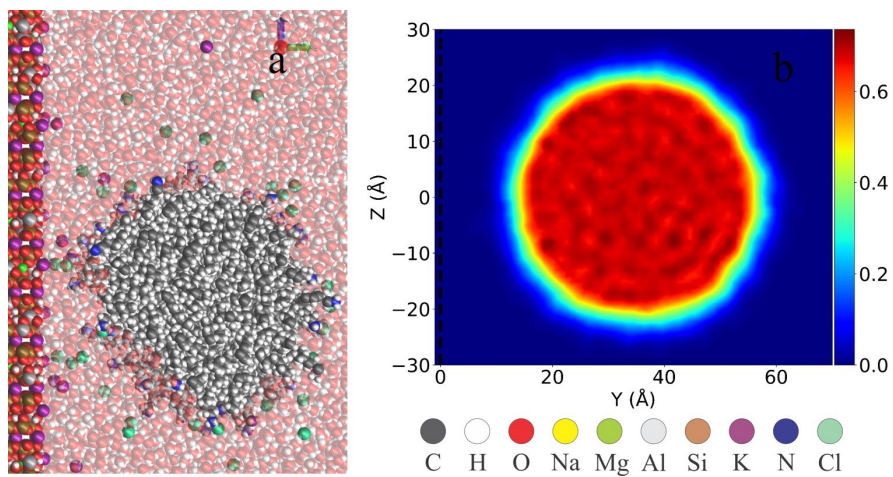


Figure S28. a) Screenshot at 8 ns of the simulation of the polar B crude oil model in water at $\text{pH} \ll 10.64$ on the edge surface. b) Corresponding density profile captured at the production stage.

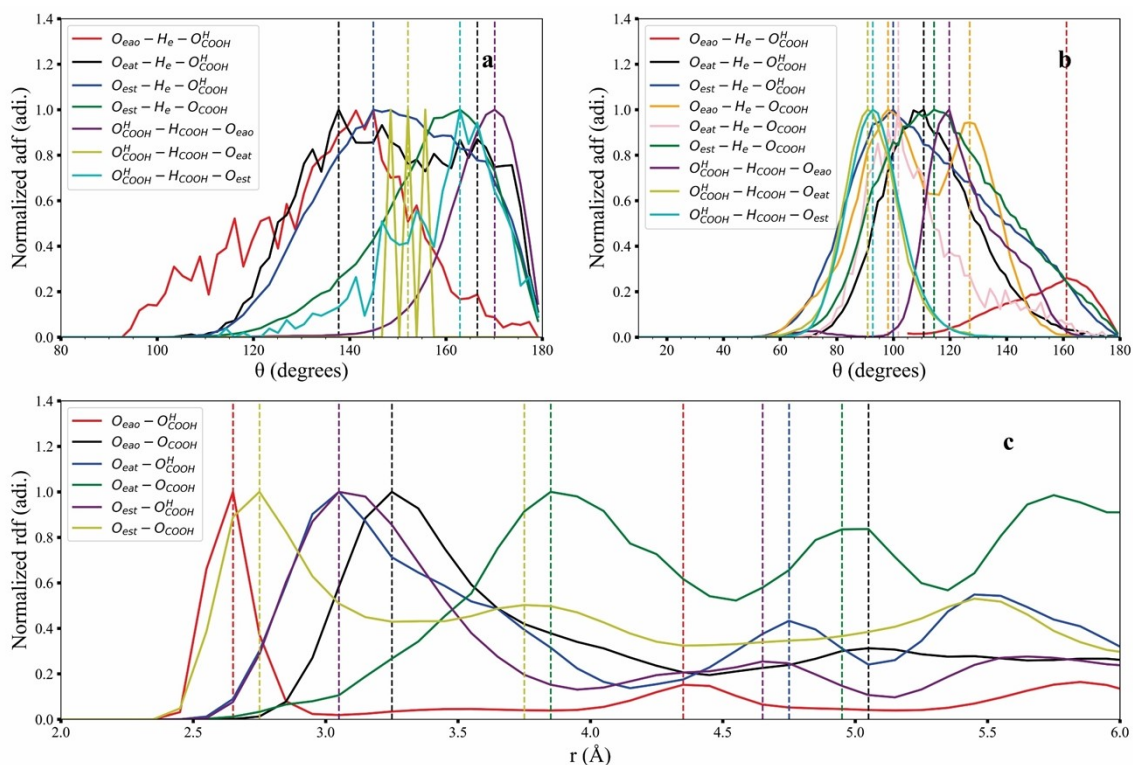


Figure S29. a) adf of the moderate hydrogen-bridging interactions between the hydroxyls of the edge surface (010) and the carboxyl group of heptanoic acid. b) adf of the weak hydrogen-bridging interactions between the hydroxyls of the edge surface (010) and the carboxyl group of heptanoic acid. c) rdf between the oxygens of the hydroxyls of the edge surface and the oxygens of the carboxyl group of heptanoic acid. The vertical lines correspond to the maxima of each curve. O_{eao} , O_{eat} and O_{est} are the edge hydroxyl oxygens attached to the octahedral aluminum, tetrahedral aluminum, and tetrahedral silicon, respectively, while H_e is the edge hydroxyl hydrogen. O_{COOH}^H , O_{COOH} , and H_{COOH} are the hydroxyl oxygen, carbonyl oxygen, and hydroxyl hydrogen of carboxyl functional group, respectively.